RES MILITARIS
REVUE EUROPEENNE D ETUDES EUROPEAN JOURNAL OF MILITARY STUDIES
Social Science Journal

Nonlinear Dynamic Response Analysis of Coastal Pile Foundation Bridge Pier Subjected to Current, Wave and Earthquake Actions: As a model of civilian live

Riyadh Alsultani1*
Department of Civil Engineering, University of Technology, 10011, Baghdad, Iraq,
Email: bce.19.52@grad.uotechnology.edu.iq

Ibtisam R. Karim
Department of Civil Engineering, University of Technology, 10011, Baghdad, Iraq,

Saleh I. Khassaf
Department of Civil Engineering, University of Basrah, 61001, Basrah, Iraq,
Email: Saleh.Khassaf@uobasrah.edu.iq

Abstract

A numerical study of the linear and nonlinear dynamic behavior of a bridge pier subjected simultaneously to water loads during earthquakes is presented. A typical coastal bridge pier with an elevated pile-cap foundation was taken as an example structure. The analysis was executed using Three-dimensional (3D) Finite Elements (FE) with localized nonlinearities in DIANA Software. It is explored how the pier's shear and moment reactions would change structurally in response to a combination of currents, waves, and earthquakes. In both the linear and nonlinear domains, the FE model's correctness was validated. The findings suggest that: (1) structural non-linearity cannot be ignored in dynamic analyses of structures in marine environments; (2) the DIANA FE model is a useful alternative approach for both linear and nonlinear dynamic analyses; and (3) structural non-linearity cannot be neglected in dynamic analyses of bridges exposed to powerful earthquakes that exceed 0.6g.

Keywords: Coastal bridge; Pile foundation; Dynamic response; Nonlinearity; Current-wave-earthquake; Diana Software.

Introduction

There is a desire for better quality and more effective transportation due to the growth of society and scientific technologies. Large-scale pile foundation bridges can offer direct connectivity between and among cities in coastal locations. They serve a crucial role in enhancing the quality of transportation as well as providing travelers with ease, which is why the building and upkeep of such bridges have received a lot of attention. When building coastal bridge constructions, two primary effects ocean waves and current loads are often taken into account. This makes sense only when doing a lengthy investigation or when the marine environment is not situated in a seismically active region. The earthquake load will take center stage in the design if the sea environment is seismically active, as it is along the eastern coast of Iraq. Therefore, the combination of earthquake pressures with sea waves and current loads poses a danger to the stability of coastal bridge constructions in seismically active coastal locations. The interaction of the vibrating pier with the surrounding water loads changes the structural vibration period and amplifies structural seismic responses during earthquakes, potentially greatly raising the risk of structural failure (Jiang et al. 2017c; Wei et al. 2011; Yang et al. 2017). There have been multiple instances in history of cross-sea pile foundation bridge demolition, which resulted in significant financial losses and negative societal effects.

In many instances, ignorance of the complexities of the offshore deepwater

environment is the primary cause of the damage (Zheng et al., 2015). A raised pile cap pile group foundation is frequently utilized to assure the strength of a coastal bridge. Due to the system's huge dimensions, complexity, and distinct three-dimensional properties, it is challenging to accurately calculate the dynamic response of a bridge foundation system under the combined effect of numerous dynamic loads using existing theories. As a result, in recent years, this topic has drawn academics who are concentrating on the dynamic behavior of offshore buildings under the combined impact of earthquakes and waves. Yamada et al. (1989) used the mode superposition method and the frequency-domain random vibration methodology to examine the dynamic behavior of offshore structures subjected to random sea waves and significant earthquake activity. Bretschneider's wave energy spectrum was used to simulate sea waves, while Kanai's power spectrum was used to simulate ground movements. A generic spectral analysis method for steel offshore buildings that were simultaneously exposed to random wave and earthquake loading processes was presented by Karadeniz (1999). The wave model's deepwater state and 3D modeling of the structure were both utilized. The random earthquake was illustrated by the ground acceleration spectrum, a variant of the well-known Kanai-Tajimi spectrum, and the random wave was expressed by a surface elevation spectrum (Pierson-Moskowitz or Jonswap).

Using ANSYS software, Abbasi et al. (2007) examined a 3D model of the Iran-Khazar Jack-up. Based on field data, the features of the marine site were determined. The Manjil earthquake in the same region served as the basis for the time-history recordings of the earthquake employed in this study. The structure-soil system was simulated using a 2D finite element analysis utilizing the ABAQUS software by Bai et al. (2008). The Taft earthquake, the El Centro earthquake, and the artificial wave from Nanjing was the earthquakes whose time-history records were employed in this study. The aforementioned estimations of hydrodynamic pressure during earthquakes often presume that the fluid is initially at rest without taking into account wave or current movements. Bridges in a marine environment may be affected by waves, currents, and earthquakes all at once. The linking mechanism of many disaster loads is not yet well understood.

Only a few studies, meanwhile, have examined the dynamic behavior of offshore buildings subjected to combined earthquake, wave, and current impacts. To analyze the dynamic reactions of fixed base offshore towers exposed to random waves and forceful earthquakes, Penzien et al. (1972) suggested a stochastic technique. Yamada et al. (1989) investigated the dynamic response of offshore structures while taking into account the interaction between the soil and the structure under the influence of random ground motions and waves. It was shown that when the tower period or water depth increased, the impact of wave force on the seismic behavior grew more significant. An experimental investigation was conducted by Zheng et al. (2015) to look at the impact of significant earthquakes and calm seas on a monopile wind turbine structure. To explore the combined effects of an earthquake, wave, and current on a pile cap cable-stayed bridge tower foundation, Liu et al. (2017) carried out an experimental investigation. Ding et al. (2018) examined the impact of wave-current interaction on the seismic behavior of a pier and the distribution law of hydrodynamic pressure along the height of the pier under various load circumstances using underwater shaking table experiments. The dynamic response of coastal structures under the simultaneous effect of earthquakes and waves, however, has only been examined thus far through experimental testing, and the findings still require the validation of numerical analysis. In order to better understand these dynamic reactions, this study looked at how offshore bridges with pile foundation piers responded to combined current-wave and earthquake effects.

Under influential earthquakes, a deep-water bridge pier may yield and enter the

nonlinear condition (Jiang et al. 2017b). Pang et al. (2015) performed fragility assessments on a multi-span deep-water bridge that was submerged in different static water depths and found that the deeper the water, the bigger the damage, most likely was. Jiang et al. (2017a) used the added-mass model to conduct fragility assessments for a deep-water bridge and discovered that the hydrodynamics might increase the risk of damage and nonlinear deformation for the analysed piers. Though it is crucial to account for both material and geometrical nonlinearity in the dynamic assessments of deep-water bridges, there aren't much research that use FE methods to solve this issue. Because of its ease and simplicity, the added-mass model has been widely utilised in design practises and research since it was originally employed by Westergaard (1933) to evaluate the hydrodynamic effect on the dam. Li and Yang (2013), Jiang et al. (2017c), and Wang et al. (2018) presented several added-mass models for deep-water cylindrical and elliptical piers. The added-mass model for the pile foundation, which is frequently utilised in practise, has, however, received less attention (Gou et al. 2018). Furthermore, the present studies regarding the verification of the added-mass model are limited to the linear seismic responses of deep-water piers; the feasibility of the added mass method in nonlinear analyses needs to be assessed.

The following steps were taken in this work to resolve issues with the dynamic behavior, structural nonlinear response, and FE model: To study the effects of joint current-wave-earthquake actions on the seismic behavior of the pier under various current speeds, wave properties, and earthquake amplitudes, three-dimensional (3D) finite element models of a prototype bridge pier with pile foundation were constructed using DIANA Software. Additionally, the linear and nonlinear responses of the example model were computed and compared, and the added-mass model was implemented in both linear and nonlinear scenarios.

Example Bridge and Numerical Model

Description of the Example Pier

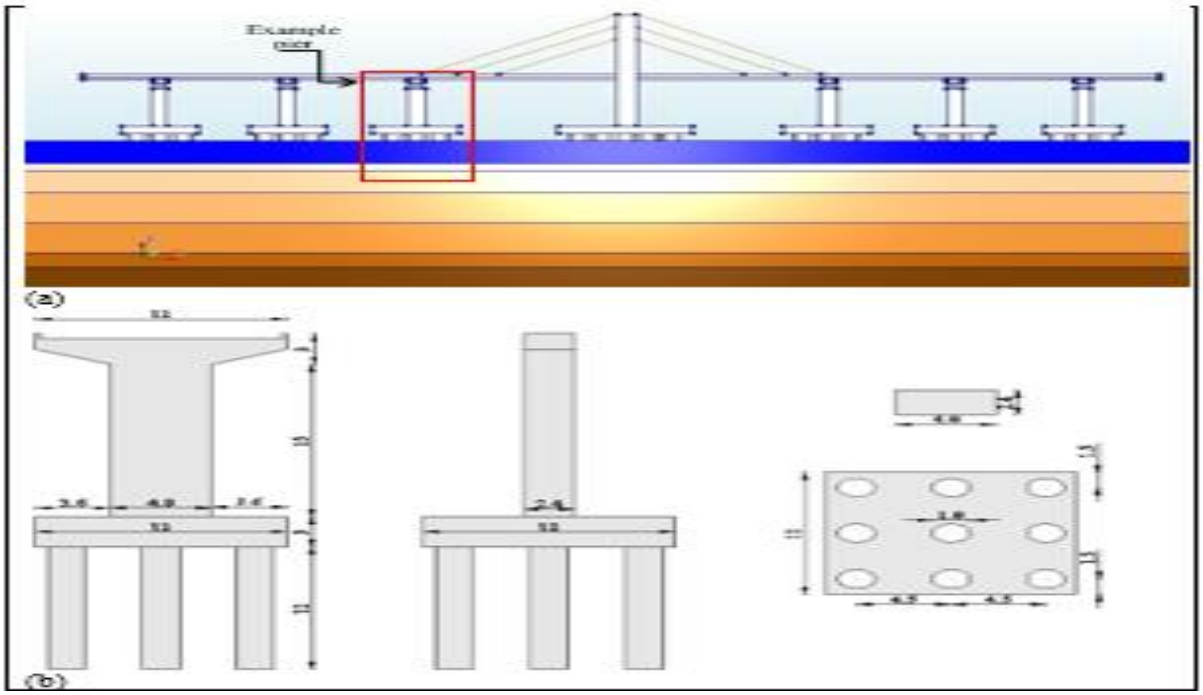

Fig. 1. *Example bridge: (a) geometry of the bridge; and (b) dimensions and details of the bridge members. All dimensions are in meters.*

The main pile foundation pier of a continuous bridge crossing the Songhua River in northeast China (Wei et al., 2013), was taken as the example bridge (Fig. 1). The example pier has a total height of 12 m with a rectangular cross-section. The foundation is composed of nine circular piles and one square pile cap. The total length of the piles is 58 m, with an assumed segment 12 m above the scour line. The bridge girder and other superstructure components were made simpler by concentrating a tip mass of 7.8x105 kg on the pier top.

Numerical Formulation

In DIANA 10.4, 2020 software, 3D solid finite elements for the piling foundation bridge pier and 3D FE for the water domain were used to create the 3D finite-element models of the pier and the surrounding water. Bridge structural dynamic response study considers the interaction of the water with the bridge as a result of the earthquake's effects, which resulted in the deformation or movement of the bridge's submerged components. The water's ability to travel is affected by the deformation or movement of these components, and the water's forces acting on the bridge took the form of hydrodynamic pressure. Eq. (1) is a more precise variant of the governing equation for transient structural dynamics (Morison et al., 1950):

$$[M]\{\ddot{x}\ (t)\} + [C]\{\dot{x}\ (t)\} + [K]\{x\ (t)\} = \{F_H(t)\} + [M]\{\ddot{x}_g\ (t)\} \quad (1)$$

Where $[M], [C]$, and $[K]$ represent the structural mass matrix, damping matrix, and stiffness matrix, respectively. $\{x(t)\}, \{\dot{x}(t)\}$ and $\{\ddot{x}(t)\}$ represent the structural relative displacement, velocity, and acceleration vectors, respectively. $\{\ddot{x}_g(t)\}$ is the acceleration vector of seismic ground motion. $\{F_H(t)\}$ is the fluid force vectors exerted on the bridge structure, including current-wave and earthquake-induced hydrodynamic forces.

The dynamic equation of motion can be represented as:

$$[M]\{\ddot{x}(t)\} + [C]\{\dot{x}(t)\} + [K]\{x(t)\} = C_M \rho V(\ddot{u} - \ddot{x}_0) + \frac{1}{2} C_D \rho A|\dot{u} - \dot{x}_0|(\dot{u} - \dot{x}_0) + \rho V\{\ddot{x}_g(t)\} \quad (2)$$

Where ρ is the water density; C_M and C_D are the coefficients of inertial and drag forces, respectively; V and A is the exposed face volume and area, respectively; $\dot{x}_0$ and $\ddot{x}_0$ are the structure absolute velocity and structure associated acceleration, respectively; and $\dot{u}$ and $\ddot{u}$ are the water velocity and water-associated acceleration, respectively.

The hydrodynamic force per unit height, P, from Eq. (2) can be presented as shown in Eq. (3):

$$P = C_M \rho A(\ddot{u} - \ddot{x}_0) + \frac{1}{2} C_D \rho B|\dot{u} - \dot{x}_0|(\dot{u} - \dot{x}_0) + \rho A\{\ddot{x}_g(t)\} \quad (3)$$

Where B is the width of the exposed face.

The first term at the right of Eq. (3) denotes the inertia force, the second term denotes the drag force, and the third term denotes structural effect.

For coastal and offshore structures, the influence of hydrodynamic drag force, represented by combined current and wave actions, on the dynamic response of structures is very important (Goto 1965; Song et al., 2013). Therefore, the Morison equation can be modified to account for currents by replacing '$\dot{u}$' by '$C + W'$, where C is the water current speed and W is wave properties and as in Eq. (4):

$$P = C_M \rho A(\ddot{u} - \ddot{x}_0) + \frac{1}{2} C_D \rho B|(C + W) - \dot{x}_0|((C + W) - \dot{x}_0) + \rho A\ddot{u} \quad (4)$$

Finite-Element Model

According to Fig. 2, the model and water were both modeled using 3D eight-node solid and eight-node FE, respectively. Due to the study's simplicity, neither the geometry of the river valley nor the impact of the nearby foundation was taken into account. To mimic how waves dissipate energy, the fluid domain was enclosed by infinite-boundary conditions [Eq. (3)]. Huang and Li specified the rigid-wall boundary condition for the bottom of the water (2011).

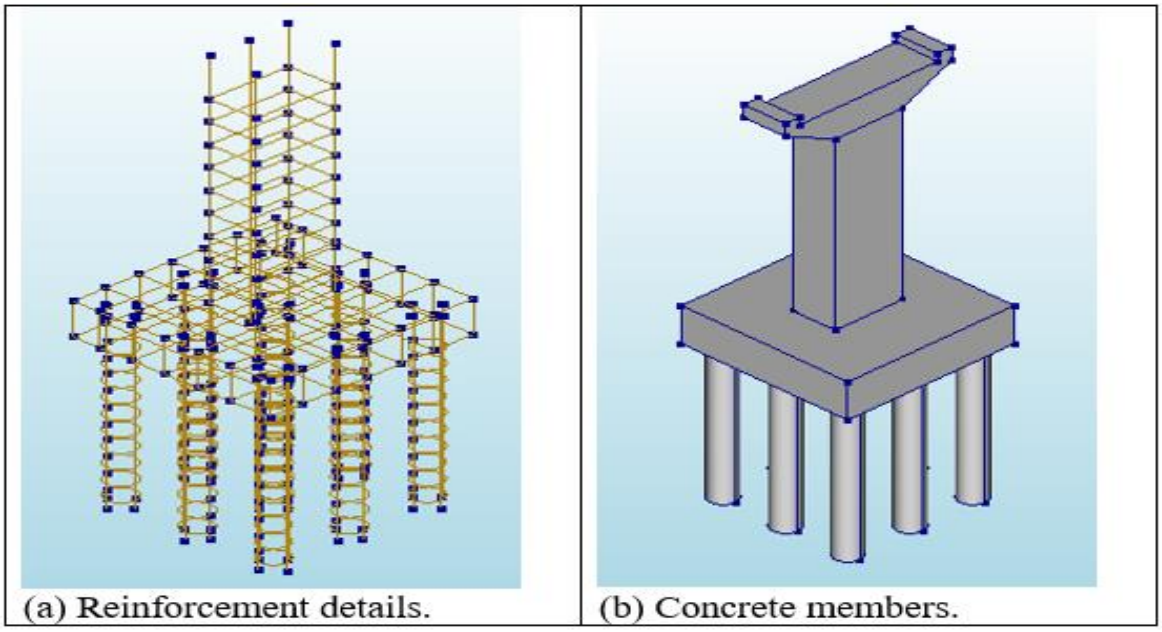
(a) Reinforcement details. (b) Concrete members.

To reproduce the model-water interaction, the model-water interaction boundary condition [Eq. (4)] was implemented to the water's surface that touches the model. In order to balance accuracy and efficiency, the meshes for the model and water were simplified into 3,616 solid elements and 354,720 finite elements, respectively. With a mass density of 1,000 kg/m3 and a compression current-wave velocity (C+W) of 1,440 m/s, it was assumed that water could be compressed. The sample model is constructed using HRB 400 rebar and C40 concrete (MCPRC 2004, Fig. 2a) (MCPRC 2004, Fig. 2b). The concrete has an elastic modulus of 32.5 GPa, a 28-day compressive strength of 34 MPa, a Poisson's ratio of 0.2, and a mass density of 2,500 kg/m3 accordingly. The rebar's elastic modulus is 210 GPa, yield strength is 400 MPa, failure strain is 0.15, and mass density is 7,850 kg/m3, accordingly. The concrete material suggested by Bathe et al. (1989), which has been validated and utilized in several prior research (Mao and Taylor 1997; Zhang et al., 2019), was employed to incorporate the influence of the concrete material's nonlinearity in the example model. The nonlinear characteristics of the RC pier were estimated using the restricted concrete model of Mander et al. to account for the contribution of the reinforcing bars to the ductility and nonlinear behavior of the reinforced core concrete (1988). According to the calculations of the confined concrete model, the elastic modulus E_c = 32.5 GPa, the maximum uniaxial compressive strength σ_c = 43.9MPa, the maximum uniaxial compressive strain e_c = 0.0049, the ultimate uniaxial compressive strength σ_u = 35.8 MPa, and the ultimate uniaxial compressive strain e_c = 0.016. The cracks were suppressed for the simulation to converge and the behavior of the concrete model in the tension zone was considered to be linear. Fig. 3 depicts the completely nonlinear stress-strain relationship of the RC material. The elastic modulus and mass density of the concrete were adjusted to constant values of 32.5 GPa and 2,500 kg/m3 for the linear studies that took into account the linear behavior of the RC material. By characterizing the kinematics of the solid element as big displacement, the influence of geometric nonlinearity was also integrated into the nonlinear analysis. The example model's seismic reactions were then computed using the created numerical models.

Fig. 2. *Finite element of the example model.*
Fig. 3. *Uniaxial stress-strain relation used in the nonlinear confined concrete material.*

Numerical Results and Discussion

Based on field data gathered in Iraq, the parameters of wave amplitude and period with a recurrence time of 50 years were determined. The fifth order Stokes wave theory is used with length 2m and period 3s. Additionally, it is predicted that the current velocity in the studied area is 2 m/s. The current and wave conditions are depicted in the Chakrabarti (1987) graphic as moderate current and short waves, respectively.

Buckling is disregarded because vertical ground acceleration is more directly connected to it (Al-Baghdadi 2014; Hameed 2019). The dynamics of marine structures are more influenced by the horizontal and vertical motions of the ground than by the pitch motion of the ground. The area under investigation uses Manjil records as its seismic history.

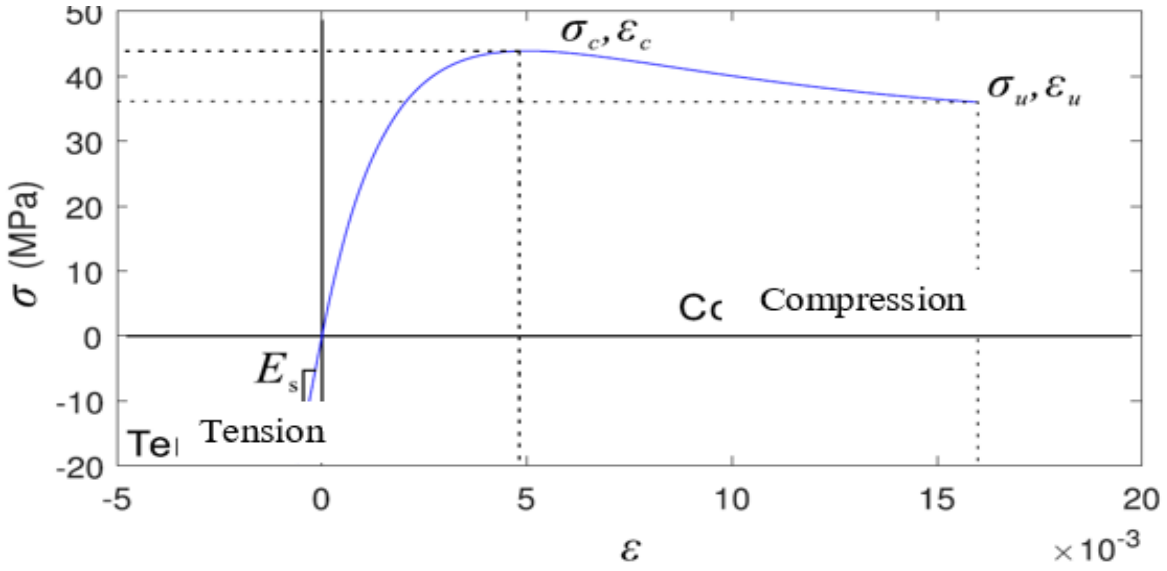

According to the Iraqi Code of Practice for Seismic Resistant Design of Buildings, the peak of time history was taken into consideration as 1.0g for the horizontal component. The acceleration time history of the Halabjah earthquake that struck Baghdad on November 12, 2017 (Al-Taie and Albusoda 2019) was chosen as the input earthquake excitation to evaluate the model structure's reaction to seismic excitation. With a peak ground acceleration (PGA) of 0.11g at 41.5 seconds, the original accelerogram had a total ground excitation time history of 205 seconds. Fig. 4 displays the amplitude spectra and acceleration time histories for the longitudinal and transverse horizontal components of this scaled earthquake excitation.

The crucial damping ratio across the frequency varied from the fundamental frequency of each model-water model to 12 Hz, and the Raleigh damping coefficients were found to be 5% of that value.

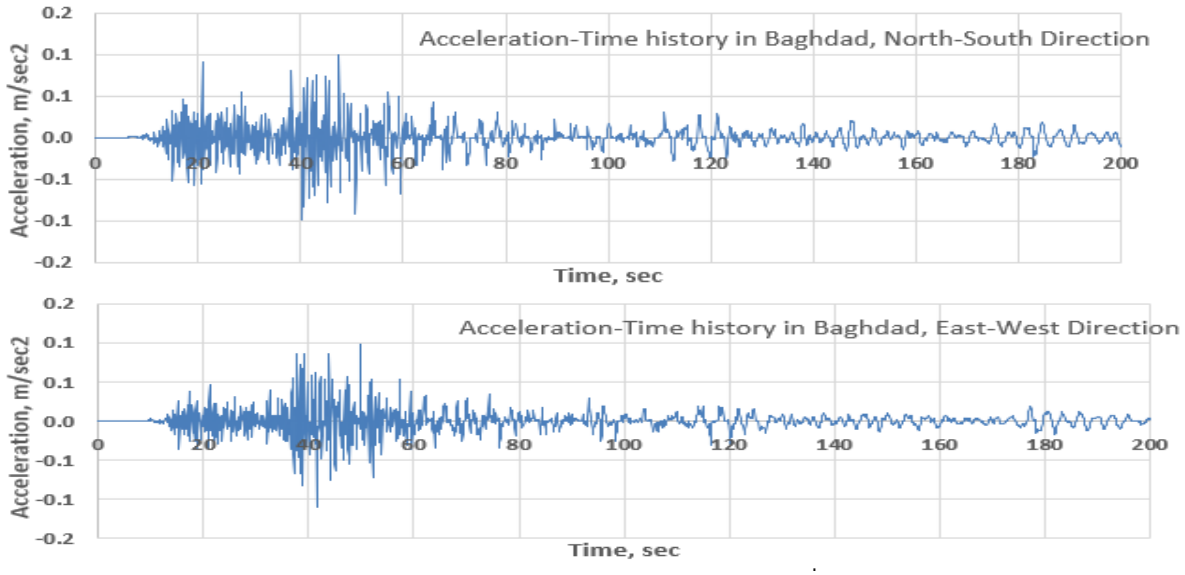

Fig. 4. *The acceleration time history of November 2017, Halabjah earthquakes in Baghdad.*

The concerns related to the dynamic behavior of the bridge pier, the consequences of structural non-linearity, and the precision of the added-mass model are covered in the next three subsections, which also serve as application examples for the created numerical model.

Dynamic Response of Bridge Pier

In order to determine whether the bridge pier is structurally stable, the absolute acceleration along the pier body and the relative displacement of the pier top to the pier bottom are both examined in the dynamic study of the bridge pier. To assess how to bridge piers were affected by the earthquake, the displacement along the pier is crucial information. The primary component affecting deck motion during a current-wave-earthquake combination is the absolute acceleration of the pier top. Fig. 5 displayed the dynamic response under the investigated factors. As can be observed, there is a fairly noticeable shift in the bridge pier's response to the relative peak displacement and peak acceleration of the pier.

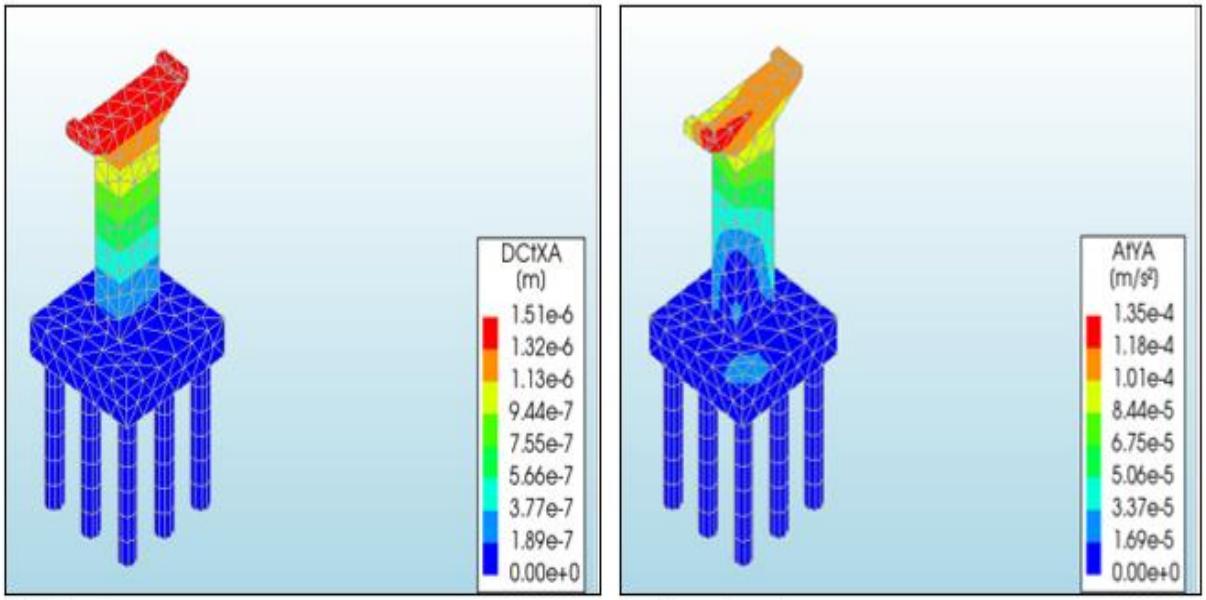

(a) Displacement response. (b) Acceleration response.

Fig. 5. *Displacement and acceleration responses of numerical model.*

Nonlinear Seismic Responses

Using a nonlinear finite element model of an example pile foundation pier exposed to coupled current-wave-earthquake activities, the impact of the model's nonlinear behavior was then investigated.

The nonlinear analysis's time step was 0.1 s, however, if an issue with convenience arises, it may be automatically split into smaller time steps.

Three water levels (12, 13.5, and 15 m), two water currents (1 and 2)m/sec, three water waves (0.4 m, 1 m, 6 sec, 0.4 m, 2 m, 3 sec, and 0.6 m, 0.1 m, 3 sec, as wave height, wave length, and wave period, respectively), six amplitude earthquake records (0.1, 0.2, 0.3, 0.4, 0.5, and 0.6 g), and a comparison of linear and nonlinear dynamic, as explained in Table (1)

Table 1. *Present study studied forces for linear and nonlinear behavior.*

Water height (m)		Water current (m/sec)		Water waves (m, m, sec)		Earthquake amplitudes (g)	
H1	12	C1	1	W1	0.4, 1, 6	A1	0.1
						A2	0.2
H2	13.5	C2	2	W2	0.4, 2, 3	A3	0.3
						A4	0.4
H3	15			W3	0.6, 1, 3	A5	0.5
						A6	0.6

As earthquake amplitudes grow from Figs. 6 to 11, either linear or nonlinear responses increasingly increase (PGA). The nonlinear responses of the pier are in good agreement with the linear responses when PGA is equal to 0.1 g. This suggests that even in such a situation, the pier was flexible. The pier entered a nonlinear condition with a rise in PGA, and its reactions were less than in linear circumstances. In particular, the nonlinear responses of base shear and base moment were much less than the linear values when PGA went up to 0.6 g.

The maximum difference between the linear and nonlinear base shear response under 0.1, 0.2, 0.3, 0.4, 0.5, and 0.6g ground motions are approximately 0%, 0.8%, 1.5%, 3.2%, 5.6 and 12%, respectively, whereas for base moment are 0%, 1.2%, 3.5%, 7.8%, 11.4 and 15%, respectively. Thus, structural nonlinearity cannot be neglected in dynamic analyses of piers subjected to strong ground motion.

The results also showed that the dynamic response of the bridge pier for linear and nonlinear base shear and base moment relative is changed in a very clear way. It can be seen that the water height, H2, 13.5m is distinguished by the increase in dynamic behavior compared with the other water heights taken in the present study. This is due to the large concrete mass affected by the applied water mass, where it can be found that the mass of the pile cap is the largest size compared to the other bridge members represented by the pier and the piles. From the foregoing, it can be concluded that the pier with a pile foundation bridge submerged in great water depths leads to a greater nonlinear deformation and the possibility of damage is higher than that of land bridges.

It can be seen that the water forces represented by currents and waves have an effect that is impossible to neglect in the case of calculating the non-linear behavior of marine structures. The effect of water currents ranges from 6% to 12%, while the effect of the waves ranged from 10% to 20%. More substantial than those under only earthquakes were the nonlinear impacts on the dynamic behavior under combination current-wave-earthquake activities. Thus, in dynamic assessments of piers susceptible to current-wave motion, particularly strong water wave action, structural non-linearity cannot be ignored. This discovery merits consideration in structural design.

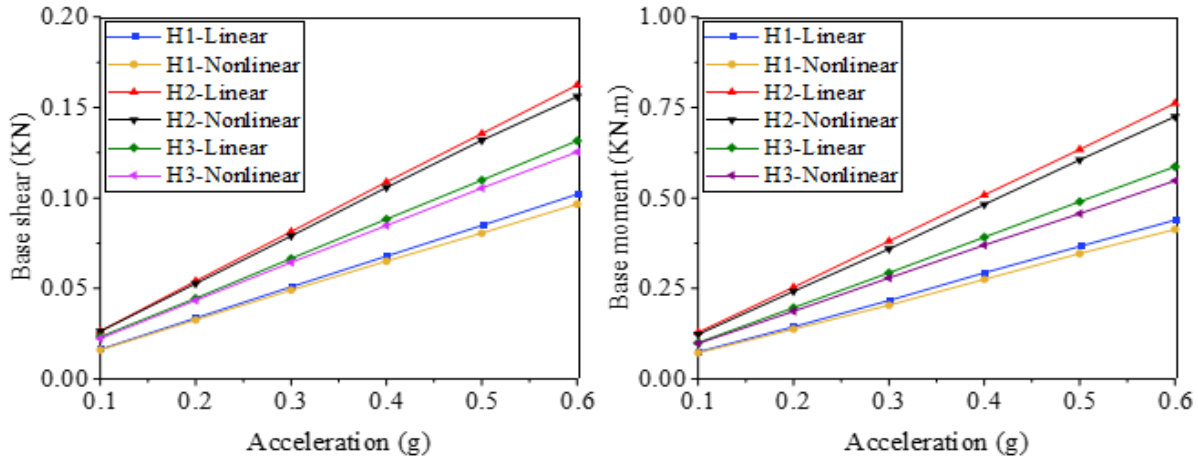

Fig. 6. *Linear and nonlinear dynamic responses (shear & moment) under C1W1.*

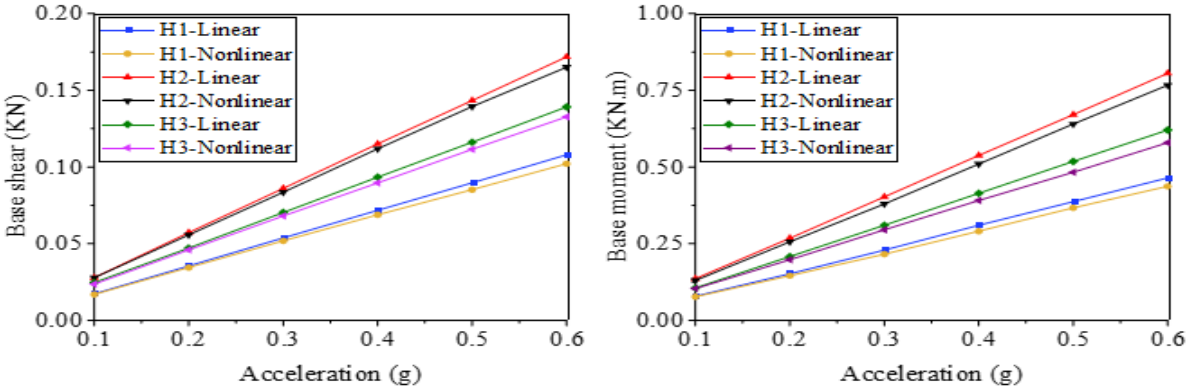

Fig. 7. *Linear and nonlinear dynamic responses (shear & moment) under C1W2.*

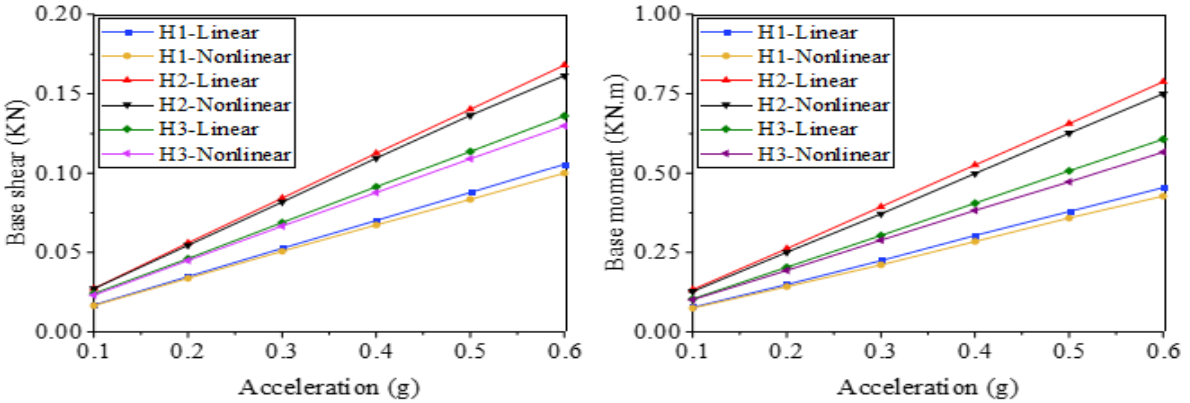

Fig. 8. *Linear and nonlinear dynamic responses (shear & moment) under C1W3.*

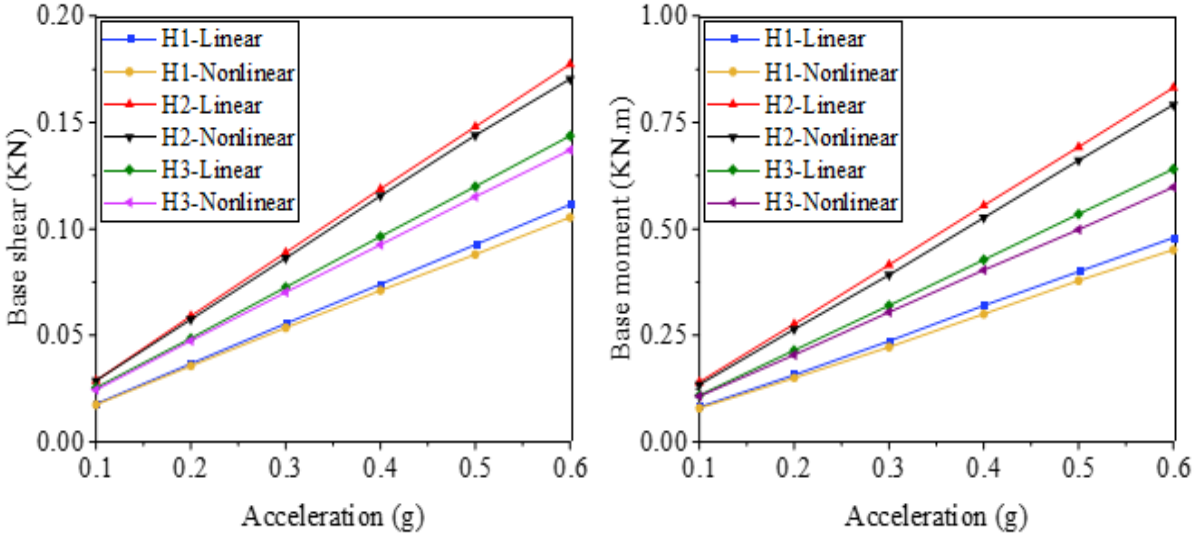

Fig. 9. Linear and nonlinear dynamic responses (shear & moment) under C2W1.

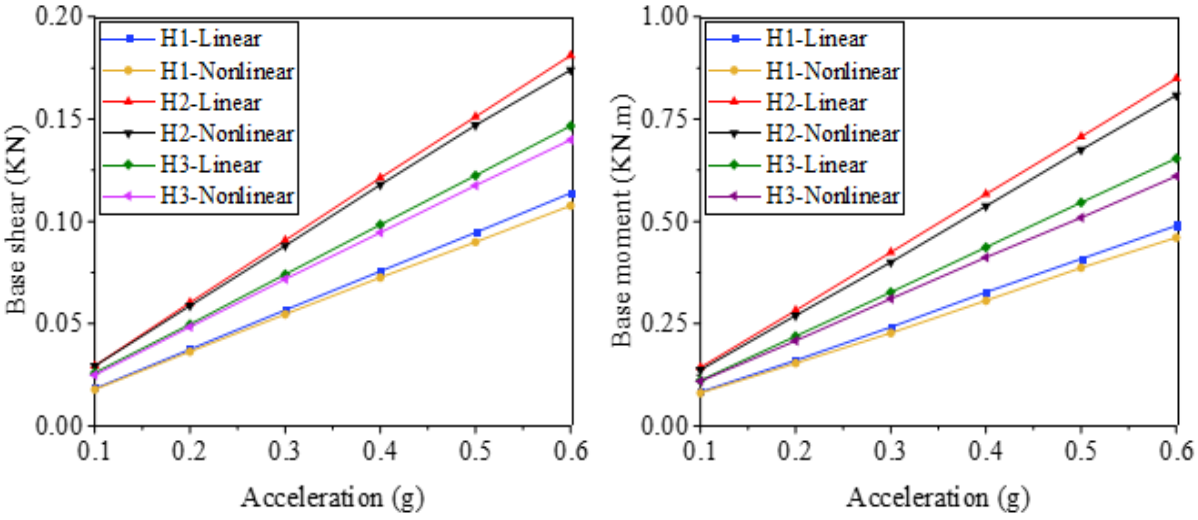

Fig. 10. *Linear and nonlinear dynamic responses (shear & moment) under C2W2.*

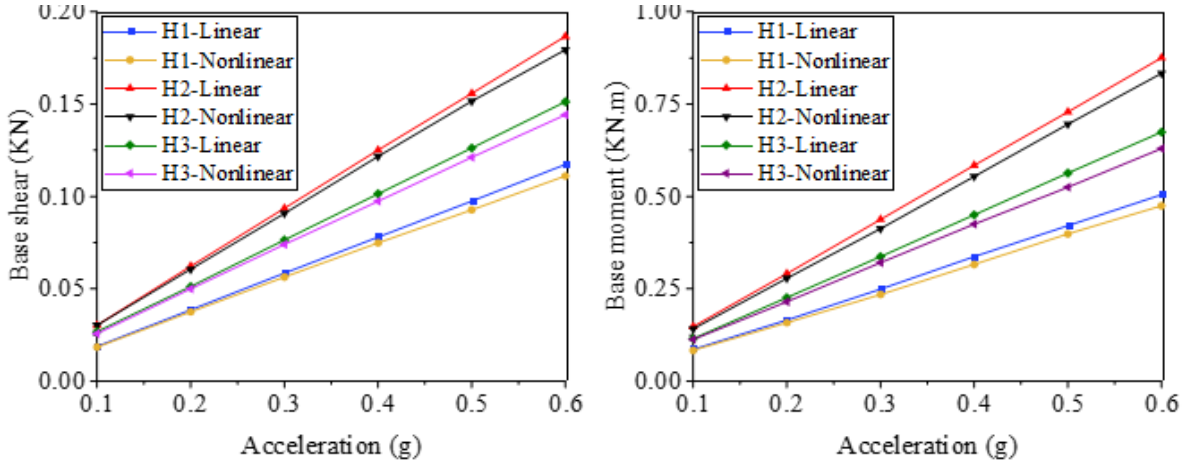

Fig. 11. *Linear and nonlinear dynamic responses (shear & moment) under C2W3.*

Validation of Added-Mass Model

Both the DIANA FE-based pile foundation bridge pier-water interaction model and the added-mass model have been used to compute the linear and nonlinear seismic responses of the example model to verify the correctness of the added-mass model. We looked at three distinct water depths: 12, 13.5, and 15 m. The ground movements for linear seismic analysis were initially assumed to be earthquakes with a scaled PGA of 0.1 g. For the nonlinear studies of the pier, these earthquakes were then scaled to ground movements with a PGA of 0.4 g. A solid-element model of the example model was used to build the added-mass model.

According to Eqs. (5)– (7), the added masses were calculated and allocated at nodes of the solid components below the still-water level (Yang 2012; Li and Yang 2013; Zhang et al., 2019).

$$M_{a0} = C_M \frac{\rho\pi B^2}{4}\left(1 - 5\frac{B}{H_w^2}\right)\left\{1 - exp\left[\frac{10(z_j - H_w)}{BH_w^{1/3}}\right]\right\} \quad (5)$$

$$M_{aI} = \rho B_1 L_1 \left\{1 - exp\left[\frac{5(z_j - H_w)}{B_1 H_w^{1/5}}\right]\right\} \quad (6)$$

$$C_M = 1.51(B/L)^{-0.17} \quad (7)$$

where M_{a0} and M_{aI} = added mass per unit length concerning outer and inner water, respectively; B and L = outside width and length of the rectangular hollow pier cross-section, respectively; B_1 and L_1 = inside width and length of the corresponding section, respectively; B and B_1 = dimensions of the sides perpendicular to the vibration direction; and z_j = vertical coordinate of Node j. The absolute maximum responses of the pier calculated by the FE and added-mass model are all scattered in Fig. 12. The linear and nonlinear behaviors, including displacement at the top of the pier, base shear, and base moment, are compared in Figs. 12(a-c) and 12(d-f). The added-mass model and the DIANA FE have an equal connection, as shown by the solid line. The result of the added-mass model is greater than the result of the DIANA model if the response point is above the solid line. The outcome of the added-mass model is smaller if this is not the case. It is evident from the comparison of the added-mass and FE models shown in Fig. 12 that, regardless of water depth, earthquake characteristics (e.g., near a fault or far field), and intensity, both the linear and nonlinear displacement at the pier top from the added-mass model agree well with those from the FE model. The added-mass model's linear and nonlinear base moments are, respectively, 0.8–1.3 and 0.9–1.2 times greater than those of the FE model. The added-mass model's linear and nonlinear base shear values are 0.8–1.3 and 0.9–1.2 times, respectively, greater than those of the FE model. Due to its high calculation efficiency, the added-mass model provided in Eqs. (5)–(7) can still be used as an alternative method to calculate the linear and nonlinear seismic responses of a pile foundation bridge pier, such as displacement at the pier top, base moment, and base shear. This is true even

though a random difference between the added mass and FE models can be found.

Fig. 12. Comparison of seismic responses of pier submerged in different water depths

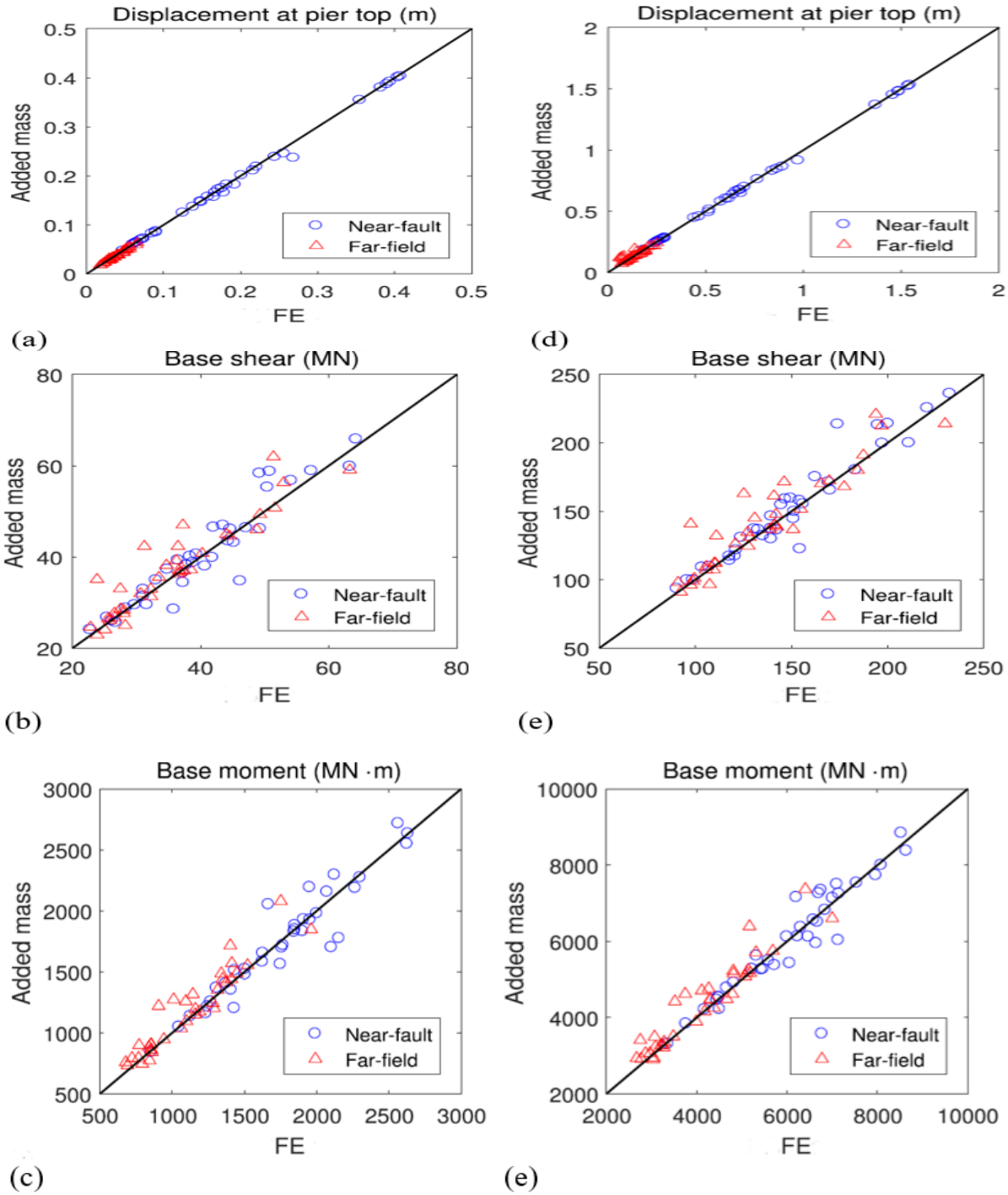

between added-mass model and FE model: (a–c) linear responses of displacement at pier top, base moment, and base shear, respectively; and (d–f) nonlinear responses of displacement at pier top, base moment, and base shear, respectively (linear responses are calculated under earthquakes with PGA of 0.1 g, whereas nonlinear responses are calculated under earthquakes with PGA of 0.4 g). The solid line indicates the equality curve between the DIANA FE and added-mass models.

Summary and Conclusions

In this work, the combined impacts of current-wave and earthquake activities on a representative pile foundation bridge pier's seismic responses were evaluated. Using DINA FE software, linear and nonlinear 3D finite-element models of the sample model-water interaction system were created. The ground motion for the linear and nonlinear seismic analysis was chosen as earthquake activity. Through comparison with the FE model, the added-mass model's correctness was confirmed. The data point to some key conclusions.

(1) The linear or nonlinear reactions progressively rise as earthquake amplitudes rise (PGA). The nonlinear responses of the pier are in good agreement with the linear responses when PGA is equal to 0.1 g. The pier entered a nonlinear condition with a rise in PGA, and its reactions were less than in linear circumstances. The nonlinear responses of base shear and base moment were much less than the linear values when PGA increased up to 0.6 g.

(2) The dynamic response of the bridge pier for linear and nonlinear base shear and base moment relative is changed in a very clear way with increases in water head. When the bridge is submerged in great water depths, this leads to a greater nonlinear deformation and the possibility of damage is higher than that of land bridges.

(3) When current waves and earthquakes were coupled, the dynamic reactions were more substantial than when earthquakes were alone. Thus, in dynamic assessments of piers susceptible to current-wave motion, particularly strong water wave action, structural nonlinearity cannot be ignored.

(4) Finally, it was discovered that irrespective of water depth, earthquake properties (near a fault or far field), and intensity, the added-mass model can be used in place of the FE model for both the linear and nonlinear seismic behavior for the example model, as well as the displacement at the pier top, base moment, and base shear.

It should be mentioned that this study still has a lot of limitations. To enhance the present model, other modeling parameters such as the geometry of the river valley, the impact of the nearby piers, and the impact of the mountains and waves warrant further investigation. It is necessary to conduct probabilistic seismic evaluations of the bridge to draw broad statistical conclusions. The numerical FE model and added-mass model confirmed in this study offer references for the hydrodynamic impacts on the seismic responses of the piled pier and can be useful for the seismic design of bridges in coastal areas, even though research on the FSI of bridges submerged in a reservoir is still far from sufficient.

Acknowledgments

Not applicable.

References

Abbasi M. and Gharabaghi A.R.M., (2007). Study the Effect of Wave Directionality on Dynamic Nonlinear Behavior of Jack-up Subjected to Wave and Earthquake Loading. 26th International Conference Shore Mechanics and Arctic Engineering, American Society of Mechanical Engineers, San Diego, pp.377–384.

Al-Baghdadi, H., (2014). Nonlinear dynamic response of reinforced concrete buildings to skew seismic excitation. Ph.D. diss., Ph. D. Thesis, Department of Civil Eng., College of Eng., University of Baghdad.

Bai D.G., Chen G.X. and Wang Z.H., (2008). Dynamic analysis of a single-column pier underground motion and wave action, World Earthquake Eng. 24 (4) (2008) 82–88.

Bathe, K.-J., J. Walczak, A. Welch, and N. Mistry, (1989). Nonlinear analysis of concrete

structures. Comput. Struct. 32 (3–4): 563–590. https://doi.org/10.1016/0045-7949(89)90347-7.

Chakrabarti, S. K., (1987). Hydrodynamics of offshore structures. WIT press.

DIANA 10.4. (2020). Theory and modeling guide. Rep. ARD 10-7, DIANA 10.4, Watertown, MA.

Ding, Y., R. Ma, Y. D. Shi, and Z. X. Li., (2018). Underwater shaking table tests on bridge pier under combined earthquake and wave-current action. Mar. Struct. 58: 301–320. https://doi.org/10.1016/j.marstruc.2017.12.004.

Goto, H., (1965). Vibration characteristics and seismic design of submerged piers. In Proc. 3-rd World Conf. Earthquake Eng., 1965 2(107-125).

Gou, H., H. Long, Y. Bao, G. D. Chen, Q. Pu, and R. Kang. 2018. Stress distributions in girder-arch-pier connections of long-span continuous rigid frame arch railway bridges." J. Bridge Eng. 23 (7): 04018039. https://doi.org/10.1061/(ASCE)BE.1943-5592.0001250.

Hameed, F., (2019). Seismic Behavior of Concrete-Steel Composite Walls. Ph.D. diss., Ph. D. Thesis, Department of Civil Engineering, College of Engineering, University of Al-Nahrain.

Huang, X., and Z. X. Li., (2011). Influence of free surface wave and water compressibility on earthquake-induced hydrodynamic pressure of bridge pier in deep water. [In Chinese.] J. Tianjin Univ. Sci. Technol. 44 (4): 319–323.

Jiang, H., B. Wang, X. Bai, and C. Zeng., (2017b). Nonlinear dynamic response character of deep-water bridge piers excited by strong near fault and far-field earthquakes. [In Chinese.] J. Huazhong Univ. Sci. Technol., Nat. Sci. Ed. 45 (8): 81–86.

Jiang, H., B. Wang, X. Bai, C. Zeng, and H. Zhang., (2017c). Simplified expression of hydrodynamic pressure on deep-water cylindrical bridge piers during earthquakes. J. Bridge Eng. 22 (6): 04017014. https://doi.org/10.1061/(ASCE)BE.1943-5592.0001032.

Jiang, H., J. M. Jin, Z. G. Wang, X. Y. Bai, and M. Wang., (2017a). Probabilistic seismic damage characteristics for piers of deep-water continuous rigid frame bridge based on IDA method. [In Chinese.] China J. Highway Transp. 30 (12): 89–100.

Karadeniz H., (1999). Spectral analysis of offshore structures under combined wave and earthquake loadings. The ninth international offshore and polar engineering conference, Brest, France.

Li, Q., and W. Yang., (2013). An improved method of hydrodynamic pressure calculation for circular hollow piers in deep water under earthquake. Ocean Eng. 72: 241–256. https://doi.org/10.1016/j.oceaneng.2013.07.001.

Liu, C., S. Zhang, and E. Hao., (2017). Joint earthquake, wave and current action on the pile group cable-stayed bridge tower foundation: An experimental study. Appl. Ocean Res. 63: 157–169. https://doi.org/10.1016/j.apor.2017.01.008.

Mander, J. B., M. J. N. Priestley, and R. Park., (1988). Theoretical stress-strain model for confined concrete. J. Struct. Eng. 114 (8): 1804–1826. https://doi.org/10.1061/(ASCE)0733-9445(1988)114:8(1804).

Mao, M., and C. A. Taylor., (1997). Non-linear seismic cracking analysis of medium-height concrete gravity dams. Comput. Struct. 64 (5–6): 1197–1204. https://doi.org/10.1016/S0045-7949(97)00029-1.

MCPRC, Ministry of Communications of the People's Republic of China. (2004). Code for design of highway reinforced concrete and pre-stressed concrete bridge and culverts. JTGD62-2004. Beijing: China Communications.

Morison, J. R., J. W. Johnson, and S. A. Schaaf., (1950). The force exerted by surface waves on piles. J. Petrol. Technol. 2 (5): 149–154. https://doi.org/10.2118/950149-G

Pang, Y., W. Kai, W. Yuan, and G. Shen., (2015). Effects of dynamic fluid structure interaction on seismic response of multi-span deep water bridges using fragility function method. Adv. Struct. Eng. 18 (4): 525– 541. https://doi.org/10.1260/1369-4332.18.4.525.

Penzien, J., and M. K. Kaul., (1972). Response of offshore towers to strong motion earthquakes. Earthquake Eng. Struct. Dyn. 1 (1): 55–68. https://doi.org/10.1002/eqe.4290010106.

Song, B., Zheng, F. and Li, Y., (2013). Study on a simplified calculation method for hydrodynamic pressure to slender structures under earthquakes. Journal of earthquake engineering, 17(5), 720-735.

Wang, P., M. Zhao, and X. Du., (2018). Analytical solution and simplified formula for earthquake induced hydrodynamic pressure on elliptical hollow cylinders in water. Ocean Eng. 148: 149–160. https://doi.org/10.1016/j.oceaneng.2017.11.019.

Wei, K., W. Yuan, and N. Bouaanani., (2013). Experimental and numerical assessment of the three-dimensional modal dynamic response of bridge pile foundations submerged in water. J. Bridge Eng. 18 (10): 1032– 1041. https://doi.org/10.1061/(ASCE)BE.1943-5592.0000442.

Wei, K., Y. J. Wu, C. Xu, Y. Pang, and W. Yuan., (2011). Numerical dynamic analysis for water-pile group bridge foundation interacted system. [In Chinese] Eng. Mech. 28 (S1): 195–200.

Westergaard, H. M., (1933). "Water pressures on dams during earthquakes." Trans. ASCE 95 (2): 418–433.

Yamada Y, Iemura H, Kawano K, Venkataramana K., (1989) Seismic response of offshore structures in random seas. Earthquake Eng. Structure. 18(7):965–81.

Yang, W., (2012). Study on hydrodynamic analysis methods of deep-water bridges. [In Chinese.] Ph.D. thesis, Southwest Jiaotong Univ.

Yang, W., Q. Li, and H. Yeh., (2017). Calculation method of hydrodynamic forces on circular piers during earthquakes. J. Bridge Eng. 22 (11): 04017093. https://doi.org/10.1061/(ASCE)BE.1943-5592.0001119.

Zhang, J., Wei, K., Pang, Y., Zhang, M., & Qin, S., (2019). Numerical investigation into hydrodynamic effects on the seismic response of complex hollow bridge pier submerged in reservoir: case study. *Journal of Bridge Engineering*, *24*(2), 05018016. https://doi/abs/10.1061/(ASCE)BE.1943-5592.0001340.

Zheng XY, Li H, Rong W, Li W., (2015). Joint earthquake and wave action on the monopile wind turbine foundation: an experimental study. Marine Structure. 44:125–41.